Low-frequency band gaps in a metamaterial rod by negative-stiffness mechanisms: Design and experimental validation

Kai Wang [1,2] , Jiaxi Zhou*[1,2] ,Qiang Wang [1,2], Huajiang Ouyang [3], and Daolin Xu [1,2]

[1] *State Key Laboratory of Advanced Design and Manufacturing for Vehicle Body, Hunan University, Changsha 410082, PR China,*

[2] *College of Mechanical and Vehicle Engineering, Hunan University, Changsha 410082, PR China,*

[3] *School of Engineering, University of Liverpool, Liverpool L69 3GH, UK*

A metamaterial rod with resonators containing negative-stiffness (NS) mechanisms is proposed for generating very low-frequency band gaps. The underlying principle is employing the NS mechanism (a pair of mutual repelling permanent magnet rings) to partially or totally neutralize the stiffness of the positive-stiffness element (two coil springs) of the resonator, and thus to achieve an ultra-low, even zero, stiffness, which enables a significant shift of the band gap from a high frequency to a low one. Experiments on the restoring force feature of the resonator and the band gap of the metamaterial rod are carried out, which provide sufficient evidence to validate the proposed concept for substantially lowering band gaps in locally resonant metamaterials. This study opens a potential path to manipulate elastic waves within a very low-frequency range.

The past two decades have witnessed a surge of conceptual designs and potential applications of elastic metamaterials, such as acoustic waveguide[1], noise control[2], inclusion cloaking[3], sound manipulation[4], and vibration isolation[5,6]. Elastic metamaterials can be built in the form of local resonance, including mass-spring devices[7–11], silicone rubber stubs[12,13], circular rubber-coated metal bars[14], beam-like structures[15], solid matrices with liquid or gas inclusions[16], rubber and metal rings[6] , and piezoelectric patches[17]. Since a locally resonant band gap is only related to the resonant frequency of the resonator, increasing the mass[16,18] and decreasing the stiffness[19,20] of the resonator are two possible approaches to lowering a band gap. However, a resonator with a traditional configuration cannot be engineered to be very heavy or very soft and hence fails to create an ultra-low frequency band gap. Consequently, generating an ultra-low frequency band gap by local resonance remains a challenge. Fortunately, the quasi-zero-stiffness isolators[21,22] have been proved to be an effective solution for passive vibration isolation, due to their high static but low dynamic stiffness, which is realized by introducing a negative-stiffness (NS) mechanism to neutralize the stiffness of the positive-

* Corresponding author

Address: College of Mechanical and Vehicle Engineering, Hunan University, Changsha 410082, PR, China.

E-mail address: jxizhou@hnu.edu.cn (Jiaxi Zhou), Tel: +86 13975835883

stiffness module. Therefore, it should be a promising way to create ultra-low frequency band gaps by engineering metamaterials with the ideal high-static-low-dynamic-stiffness (HSLDS) feature [6,19,23,24].

In this letter, a local resonator is explored by connecting a pair of mutual repelling permanent magnetic rings with two coil springs in parallel, as shown in Fig. 1. The negative stiffness arising from the magnet rings is employed to counteract the positive stiffness provided by the coil springs, leading to ultra-low (even zero) stiffness. However, the load-bearing capability of the resonator is not influenced by the NS mechanism, because the rated load is totally supported by the coil springs at the static equilibrium position. Hence, this resonator is called HSLDS resonator here. A detailed description of the configuration is presented in the supplementary material (SM). This HSLDS resonator is particularly interesting because it can manipulate a longitudinal wave along a metamaterial rod (meta-rod) in a much lower frequency range than a traditional local resonator. A prototype of this subwavelength metamaterial rod with such resonators is built, and the underlying mechanism for lowering band gap frequency by the NS mechanism is experimentally validated. This work provides a perspective for the design of low-frequency elastic metamaterials based on the concept of the NS mechanism, which could be exploited in a wave filter for attenuation of ultra-low frequency vibration.

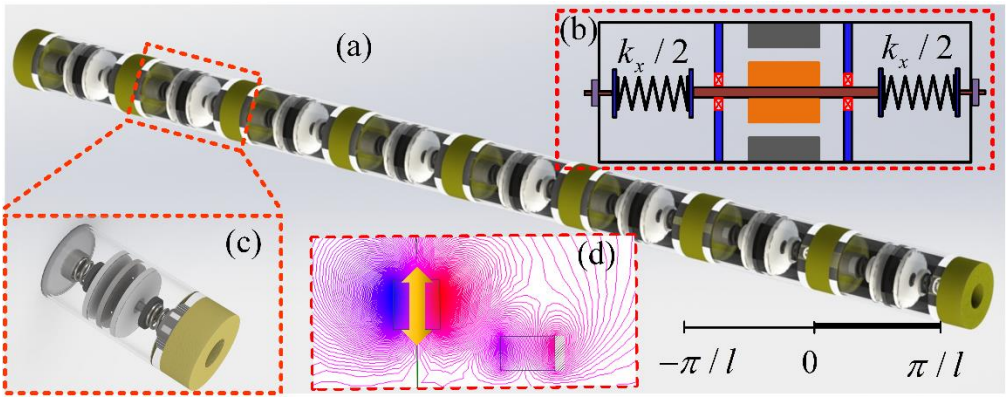

FIG. 1. (a) Schematic diagram of the meta-rod, (b) the computational model of the local resonator, (c) the unit cell of the meta-rod and (d) the distribution of the magnetic flux lines of the permanent magnet springs. The yellow hollowed cylinders in (a) and (c) represent rubber rings, and the orange and dark grey parts in (b) represent the inner and outer magnet rings, respectively.

When the resonator is at its static equilibrium position, as shown in Fig. 1 (b), the NS mechanism is not active. When an external force is applied on the resonator, the inner magnet ring connected with the guide-bar moves away from its static equilibrium position by a distance x. Because the guide-bar

is supported by two sliding bearings and both coil springs are compressed by screws, the guide-bar can move with very low friction and keep contact with the coil springs throughout the full range of motion. It should be noted that the inner and outer permanent magnets are magnetized axially. The magnetic flux lines obtained by finite element analysis are exhibited in Fig. 1 (d). When the inner magnet ring leaves the static equilibrium position, a repulsive force $F_{\mathrm{NS}}(x)$ arising from the NS mechanism acts on the guide-bar. The detailed static analysis can be found in Section II of SM. Since both the guide-bar and the inner permanent magnet ring are constrained to move along the axial direction, only the axial repulsive force between the inner and outer magnet ring is considered, and the restoring force can be given by $F_{\mathrm{HSLDS}} = k_x x - F_{\mathrm{NS}}(x)$. Differentiating the restoring force with respect to the distance *x*, the stiffness of the resonator can be derived as $K_{\mathrm{HSLDS}} = k_x - k_{\mathrm{NS}}(x)$, where $k_{\mathrm{NS}}(x)$ is the stiffness of the NS mechanism. It is clear that the stiffness of the coil spring is neutralized by the permanent magnet rings.

Based on the design concept of the NS mechanism, the unit cell for the meta-rod is fabricated and all the geometrical parameters are listed in Table S1 of SM. The stiffness coefficients of the coil springs are measured experimentally, which show that they are slightly different from each other in the range of $(1.9\sim2.1)\times10^4$ N/m, due to machining and assembly errors. In order to conduct the following theoretical analysis of the metamaterial rod, the average value 2×10^4 N/m is taken as the stiffness coefficients. To measure the restoring force of the resonator, one of the two coil springs is removed, as shown in Fig. 2 (a). By pressing the handle of the measuring instrument with different amounts of compression, and recording the displacements and restoring forces from the display screens, the relationship between the restoring force and the displacement can be obtained. The measured displacements are subtracted by a displacement (3.76 mm) to shift the origin of coordinate from the original position of the inner magnet ring to the static equilibrium position, as shown in Fig. 2(b). Additionally, the measured results only include the forces provided by only one coil spring and the NS mechanism. However, the stiffness of the coil spring is linear, and thus, the stiffness of the resonator can be achieved by adding the stiffness of one coil spring onto the measured stiffness.

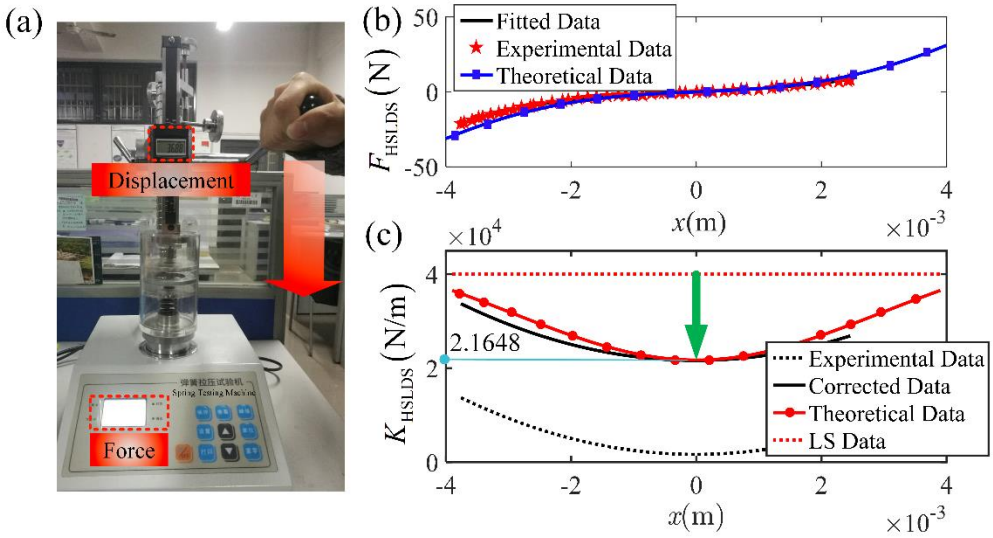

FIG. 2. (a) Experimental setup for testing the restoring force of the resonator, (b) experimental, fitted and theoretical forces and (c) experimental, corrected and theoretical stiffness. The stiffness of the corresponding linear resonator is also presented in (c) with red dotted line and legend "LS Data".

As shown in Fig. 2 (b), the restoring force calculated from the analytical expression (Eq. S5 in SM) are shown by the blue solid line with rectangles, and the measured data for the restoring force (red pentagrams) are fitted as a 5th-order polynomial (the black solid line). Differentiating the fitted polynomial with respect to the displacement x, the experimental stiffness (black dotted line) is obtained, as shown in Fig. 2 (c). And then, the stiffness of the resonator is achieved by adding the stiffness of the coil spring (2×10^4 N/m), which is depicted as black solid line in Fig. 2(c). The theoretical stiffness of the resonator and the linear resonator without the NS mechanism are also presented in Fig. 2(c) by the red solid line with dots and the red dotted line, respectively. Clearly, the experimental stiffness matches well with the theoretical one near the static equilibrium position, while it deviates from the theoretical one as the displacement increases. Such a difference is caused by possible manufacturing and assembling errors of the magnet rings. From this figure, it can be seen that the stiffness of the resonator is reduced effectively by the magnet rings from 4×10^4 N/m to 2.1648×10^4 N/m at the static equilibrium position. With the increase in the displacement x, the contribution of the NS mechanism gradually declines. Therefore, as depicted in Fig. S3 in SM, the stiffness of the resonator reaches its minimum value γk_x at the static equilibrium position, which is a typical feature similar to a quasi-zero stiffness system [25].

Furthermore, the metamaterial rod is modelled as a lumped mass-spring chain (as shown in Fig.

S5) to theoretically predict the band gaps. The linearized stiffness γk_x ($0 \le \gamma \le 1$) is utilized to derive the theoretical dispersion relations as long as the vibration amplitude is not large[6,23,24]. The mass of the resonator m is composed of the masses of the guide-bar, the inner permanent magnet ring and two support plates which are fixed on the guide-bar. The mass of the host structure M includes the masses of the acrylic cylinder and the outer permanent magnet ring. The rubber ring is modelled as a spring with stiffness K [19]. By using the Harmonic balance method, the dispersion relation of the lumped mass-spring chain can be given by [26]

$$\cosh(lq) = 1 + \frac{\Omega^4 - (\nu + \beta)\gamma\Omega^2}{2(\nu\gamma - \Omega^2)} \tag{1}$$

where l is the lattice constant, q the wave vector of the longitudinal wave, $\Omega = \omega / \omega_0$ ($\omega_0 = \sqrt{k / M}$) is non-dimensional frequency, and $\nu = \beta / \alpha$ ($\alpha = m / M$, $\beta = k / K$). The detailed derivation of Eq. (1) is presented in Section III of SM. Note that the damping and the nonlinearity of the resonator are not considered in the theoretical analysis. For the lumped mass-spring chain, the beginning and ending frequencies of the band gap can be given by $\omega_1 = \sqrt{\gamma k_x / m}$ and $\omega_2 = \sqrt{\gamma k_x (M + m) / Mm}$, respectively, and the bandwidth can be calculated as $\Delta\omega = \omega_2 - \omega_1$. When the frequency locates in the region of $\omega_1 < \omega < \omega_2$, the longitudinal wave propagation is hindered. Clearly, the location of the band gap can be influenced by the stiffness of the linear spring, the mass of the resonator and the net stiffness ratio γ. Interestingly, the beginning frequency of the band gap is reduced from $\sqrt{k_x / m}$ to $\sqrt{\gamma k_x / m}$ after the pair of permanent magnet springs, acting as the NS mechanism, is switched on, leading to a desired low frequency band gap.

To assess the advantage of the meta-rod with NS mechanism, the dispersion relation Eq. (1) is solved for a given frequency, and then a complex solution of the propagation constant ql is obtained. For the lumped mass-spring chain, the displacement of the nth mass of the host structure can be written as the lattice wave solution $u_n = A\mathrm{e}^{\mathrm{i}(nql - \omega t)}$. Assuming $ql = p_1 + \mathrm{i}p_2$ and substituting it into the lattice wave solution of the nth lumped mass yields

$$u_n = A\mathrm{e}^{-np_2}\mathrm{e}^{\mathrm{i}(np_1 - \Omega t)} \tag{2}$$

where A denotes the amplitude of the displacement. The imaginary part of the propagation constant

(ql) represents the wave attenuation along the meta-rod, and thus it is named as attenuation constant. With the increase in its imaginary part, the wave attenuation in the band gap region gets enhanced. In addition, its real part is named as phase constant, which determines the phase of the wave propagation. The theoretical band structure of the meta-rod influenced by the geometrical parameters of the NS mechanism is presented in Fig. S6 and Fig. S7 in SM. With the increase of the height of the magnet ring and the decrease of the air gap between the inner and outer magnet rings, the net stiffness ratio decreases and the band structure moves to a low-frequency region. This implies that the NS mechanism, a pair of mutually repealing magnet rings, can markedly lower the band gap and thus attenuate the low-frequency longitudinal wave.

To validate the theoretical predictions of the band structure, and also to show the advantage of the meta-rod with the NS mechanism, a prototype of this meta-rod consisting of 7 unit cells with a lattice constant l=0.163 m is fabricated. The experimental setup is shown in Fig. 3 (a) and the resonator mass m and the lumped mass of the host structure M are 0.062 kg and 0.598 kg, respectively. The stiffness of the rubber is $K = 493.7842$ N/mm .

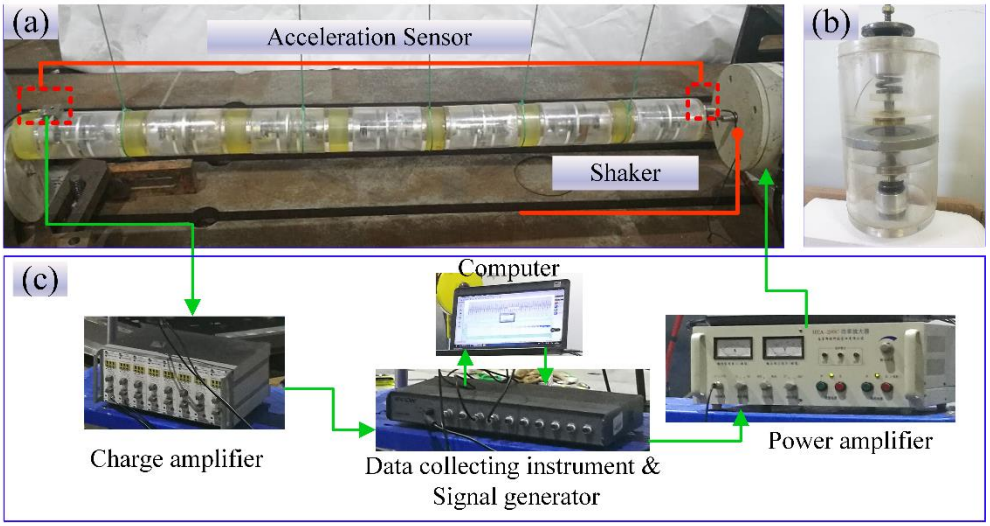

FIG. 3. Experimental setup of (a) the meta-rod, (b) the unit cell and (c) the measurement setup for acceleration acquisitions.

The edge frequencies of the band gap are calculated by employing the undamped lumped mass-spring model with linearized stiffness for different net stiffness ratios. As shown in Fig. 4, the white dotted lines represent the edge frequencies, which enclose a region for the band gap. Within this region, as the imaginary part of the wave propagation constant ql increases, the colour becomes bright, which implies that the wave attenuation gets better. Specifically, the bandwidths (the black axis in the subplot)

and the real part of ql (the red axis in the subplot) are illustrated in the bottom right corner, when the net stiffness ratio is 0.5 (a half of stiffness of the resonator is neutralized by the permanent magnet rings) and 1 (the permanent magnet rings are removed), respectively.

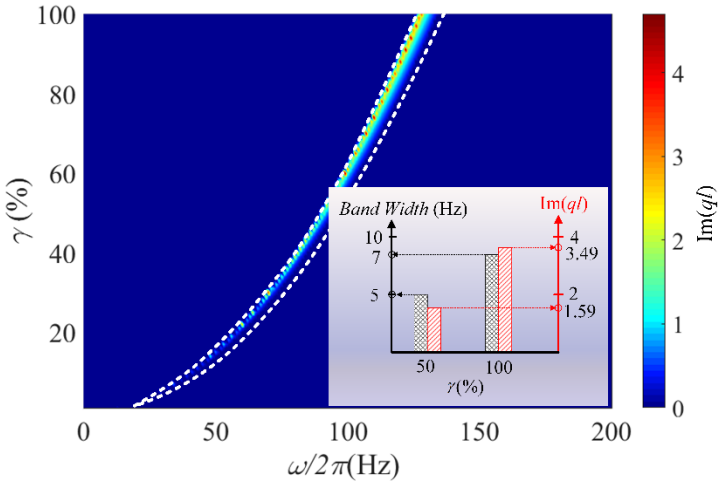

FIG. 4. Band structure of the meta-rod with different net stiffness ratios. The bottom right corner shows bandwidths and imaginary parts for two special cases when the net stiffness ratio is selected as γ=0.5 and γ=1.

From Fig. 4, it is clear that with the decrease in the net stiffness ratio, the band gap moves into a low-frequency region. Specifically, when the net stiffness ratio decreases from 1 to 0.01, the beginning frequency of the band gap shifts from 127 Hz (the resonant frequency of the linear resonator without the NS mechanism) to 13 Hz, which exhibits a notable advantage of the NS mechanism for effectively neutralizing the stiffness of the linear spring and thus substantially reducing the net stiffness of the resonator. And it also verifies the theoretical prediction that the beginning frequency can be decreased from ω_0 to $\omega_0\sqrt{\gamma}$. However, with the decrease in the beginning frequency, the bandwidth becomes narrow and the wave attenuation gets less effective. For local resonant metamaterials, it is still a challenge to obtain an ultra-low frequency band gap with a wide bandwidth.

In the experimental setup, one end of the meta-rod is connected to a shaker, which provides a harmonic excitation over a broadband frequency range along the axial direction of the meta-rod. Two acceleration sensors are attached at both ends of the meta-rod to record the dynamic responses in the axial direction. The details about the test equipment are presented in Table S2 in the SM. Note that both the meta-rod and the shaker are suspended by flexible strings to simulate the free-free boundary condition. The right-hand end of the meta-rod is fixed with a rubber ring to eliminate the effect of the

rigid-body motion. The transmittance is computed as the ratio between the output (left-hand) and input (right-hand) acceleration signals, which is defined by $20\log_{10}\|A_{out}(\omega)/A_{in}(\omega)\|$.

The imaginary and real parts of the wave propagation constant calculated by the Harmonic balance method by using the lumped mass-spring model are depicted in Fig. 5 (a) and Fig. 5 (b), respectively, where the shaded area denotes the band gap. It is clear that compared with the real part, the imaginary part can represent the band structure more completely, including the bandwidth, the central frequency and wave attenuation within the band gap.

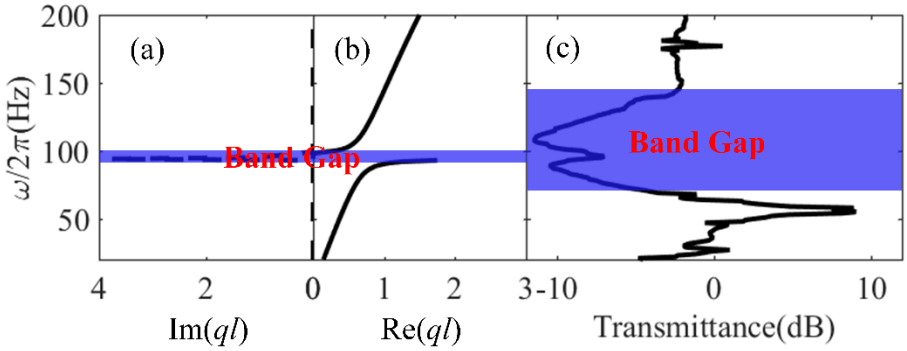

FIG. 5. Comparison of the band structure predicted theoretically by Harmonic Balance method with that by experimental transmittance.

By forward frequency sweep testing, the accelerations of the first and last unit cells of the meta-rod are obtained, and then the acceleration transmittance can be calculated, as shown in Fig. 5 (c). Obviously, the transmittance curve has two sharp drops at 89 Hz and 109 Hz, which are considered as two band gaps [27], which does not match the theoretical prediction (only one band gap at 94 Hz). It can be attributed to a fact that the stiffness coefficients of the linear springs and NS magnet springs might be somewhat different from each other due to machining errors, leading to different resonant frequencies for each resonator, and thus bring about multiple band gaps [28]. More importantly, these multiple band gaps with close central frequencies can merge into an ultra-wide band gap, as shown by the shade area in Fig. 5 (c). In addition, the damping from materials and the friction in the experimental setup are another reason for the widening of the band gap [6].

In conclusion, this letter proposes a metamaterial rod (meta-rod) for a very low-frequency band gap by introducing the NS mechanism into the linear resonator. The NS mechanism is realized by using a pair of mutually repelling permanent magnet rings. The experimental prototype of the meta-rod is fabricated, and the stiffness of the HSLDS resonator is measured by experimental testing. Both the

theoretical and experimental results show that the stiffness of the resonator can be reduced effectively by the NS mechanism, which validates the design concept of the HSLDS resonator. Furthermore, the meta-rod is modelled as a lumped mass-spring chain, and the theoretical dispersion relation is derived by using the Harmonic balance method. The results exhibit that the band gap is substantially shifted from a high-frequency region to a low one with increasing NS stiffness, which are also validated by experimental results. Therefore, the metamaterials with HSLDS resonators should be a promising solution to manipulate elastic waves within a very low-frequency region. Most interestingly, the measured bandwidth of the meta-rod prototype is much wider than the theoretical predication, probably due to the mismatching resonant frequencies for each resonator, which lights the realization of wide ultra-low band gaps by employing the HSLDS resonators with mismatching stiffness.

See supplementary material for details on the configuration and parameters of the metamaterial rod, static analysis of the resonator, and theoretical band structures.

This research work is supported by National Key R&D Program of China (2017YFB1102801), National Natural Science Foundation of China (11572116) and Hunan Provincial Innovation Foundation for Postgraduate. The first author, Kai Wang, would like to thank the support from the China Scholarship Council (CSC) which sponsors his visit to the University of Liverpool where the major theoretical part of this research is conducted.

[1] A. Khelif, A. Choujaa, S. Benchabane, B. Djafari-Rouhani, and V. Laude, Appl. Phys. Lett. **84**, 4400 (2004).
[2] T. Elnady, A. Elsabbagh, W. Akl, O. Mohamady, V.M. Garcia-Chocano, D. Torrent, F. Cervera, and J. S ánchez-Dehesa, Appl. Phys. Lett. **94**, 2007 (2009).
[3] L. Zigoneanu, B.I. Popa, and S.A. Cummer, Nat. Mater. **13**, 352 (2014).
[4] C. He, X. Ni, H. Ge, X.C. Sun, Y. Bin Chen, M.H. Lu, X.P. Liu, and Y.F. Chen, Nat. Phys. **12**, 1124 (2016).
[5] J. Mei, G. Ma, M. Yang, Z. Yang, W. Wen, and P. Sheng, Nat. Commun. **3**, 756 (2012).
[6] K. Wang, J. Zhou, X. Daolin, and H. Ouyang, J. Phys. D. Appl. Phys. **52**, 055104 (2019).
[7] X. Fang, J. Wen, D. Yu, and J. Yin, Phys. Rev. Appl. **10**, 054049 (2018).
[8] D. Yu, Y. Liu, H. Zhao, G. Wang, and J. Qiu, Phys. Rev. B - Condens. Matter Mater. Phys. **73**, 064301 (2006).
[9] E.J.P. Miranda, E.D. Nobrega, A.H.R. Ferreira, and J.M.C. Dos Santos, Mech. Syst. Signal Process. **116**, 480 (2019).
[10] M.Y. Wang and X. Wang, J. Phys. D. Appl. Phys. **46**, 255502 (2013).
[11] K. Wang, J. Zhou, C. Cai, D. Xu, and H. Ouyang, Appl. Math. Model. **73**, 581 (2019).
[12] M. Oudich, M. Senesi, M.B. Assouar, M. Ruzenne, J.H. Sun, B. Vincent, Z. Hou, and T.T. Wu, Phys. Rev. B - Condens. Matter Mater. Phys. **84**, 165136 (2011).
[13] M. Oudich, M.B. Assouar, and Z. Hou, Appl. Phys. Lett. **97**, 193503 (2010).
[14] Y.F. Wang, Y.S. Wang, and V. Laude, Phys. Rev. B - Condens. Matter Mater. Phys. **92**, 104110 (2015).
[15] X. Wang and M.Y. Wang, Meccanica **51**, 171 (2016).

[16] Q. Zhang, K. Zhang, and G. Hu, Appl. Phys. Lett. **112**, 221906 (2018).
[17] B. Bao, D. Guyomar, and M. Lallart, Mech. Syst. Signal Process. **82**, 230 (2017).
[18] Z. Wang, Q. Zhang, K. Zhang, and G. Hu, Adv. Mater. **28**, 9857 (2016).
[19] K. Wang, J. Zhou, D. Xu, and H. Ouyang, Mech. Syst. Signal Process. **124**, 664 (2019).
[20] O.R. Bilal, A. ́e Foehr, and C. Daraio, Proc. Natl. Acad. Sci. U. S. A. **114**, 4603 (2017).
[21] X. Sun, J. Xu, X. Jing, and L. Cheng, Int. J. Mech. Sci. **82**, 32 (2014).
[22] Z. Hao, Q. Cao, and M. Wiercigroch, Nonlinear Dyn. **87**, 987 (2017).
[23] J. Zhou, K. Wang, D. Xu, and H. Ouyang, J. Appl. Phys. **121**, 044902 (2017).
[24] J. Zhou, K. Wang, D. Xu, and H. Ouyang, Phys. Lett. Sect. A Gen. At. Solid State Phys. **381**, 3141 (2017).
[25] K. Wang, J. Zhou, and D. Xu, Int. J. Mech. Sci. **134**, 336 (2017).
[26] B.S. Lazarov and J.S. Jensen, Int. J. Non. Linear. Mech. **42**, 1186 (2007).
[27] Y. Xiao, J. Wen, and X. Wen, J. Phys. D. Appl. Phys. **45**, 195401 (2012).
[28] S. Zhang, J. Hui Wu, and Z. Hu, J. Appl. Phys. **113**, 163511 (2013).